Proceedings of Engineering & Technology (PET)
pp. 766-771

A Comparison of Slices Images Segmentation for the 3D MRI Denoising Methods

Feriel Romdhane[#1], Faouzi Benzarti[#2], Hamid Amiri[#3]

[#]LR-SITI, National Engineering School of Tunis, El Manar University
[#]Campus Universitaire, B.P.37, 1002 Tunis, Belvédère, Tunisie.

[1]feriel.romdhane@enit.rnu.tn
[2]benzartif@yahoo.fr
[3]hamidlamiri@gmail.com

***Abstract*— Noise removal is a vital role in medical imaging, such as in magnetic resonance imaging (MRI). So in order to preserve the important features and to guarantee the correct diagnosis, the authors have proposed a new method for removing noise based on NL-mean filter and diffusion tensor. This paper presents a comparison of the MRI slices images segmentation extracted from a some 3D denoised techniques and our proposed algorithm, by using two common methods such as the Fuzzy c-means and Kmeans clustering. Some quantitative measures are used to evaluate the performance of such as methods.**

***Keywords*— 3D MRI, Noise removal, Segmentation, Fuzzy c-means, Kmeans**

I. Introduction

The Magnetic resonance imaging (MRI) is a medical imaging technique used to diagnose and treat medical conditions by imaging the anatomy and the physiological processes of the body in both health and disease. These images are subject of a common noise called Rician noise [1] which is a signal-dependent allows to reduce the image contrast and causes random fluctuations. The removing noise is a necessary task for this kind of images in order to preserve the important features and to guarantee the correct diagnosis. In literature, many noise removal algorithms was applied successfully for MRI such as the wavelet transform [1][2], the variational algorithms [3][4], the anisotropic diffusion filtering [5][6][7][8] and the Non-Local Means (NLM) algorithm [10][11][12]. Previously we proposed a new method for removing noise based on combination between the NL-mean filter and the anisotropic diffusion tensor [15]. On the one hand, the NL-mean filter is based on a weighted average based on the Euclidean distance of voxels inside a search window in image, and in the other hand, the anisotropic diffusion tensor is based on the nonlinear partial differential equation (PDE) proposed by Weickert [8] depends on the position and the orientation of the pixel which preserves important features such as edges and discontinuities. Moreover, the image segmentation is one of the most important stage in medical image which partitioning measuring pathological regions. In literature, many segmentation methods were developed for the MRI data among these methods: Kmeans [13] and Fuzzy c-means [14] clustering was widely applied for the MRI segmentation.

In this paper, we present a comparison of MRI slices segmentation using two common methods such as the Fuzzy c-means and Kmeans clustering, denoised previously by our proposed algorithm and other 3D common removal noise methods. The paper is organized as follows: In section 2, we introduce the proposed removing noise algorithm. Section 3 defines some common segmentation algorithms. Section 4 presents results in terms of denoising and segmentation; and section 5 concludes the work.

II. Our Previous Work

In our previous work for the 3D MRI denoising [15], we have proposed a new method based on combination between two filters such as the non local mean filter and the anisotropic diffusion tensor with an estimator noise Rician in order to preserve structures in 3d data [12].

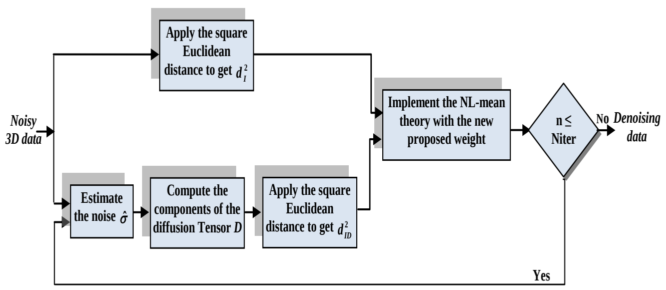

Fig. 1 The Proposed algorithm in the previous work [15].

So, we modified the weight average of the NL-mean filter by the as following equation:

$$w(x_i,x_j)=\frac{1}{Z(x_i)}e^{-\left(\frac{d_I^2(x_i,x_j)+d_{ID}^2(x_i,x_j)}{h}\right)^2} \quad (1)$$

Where:

$d_I^2(x_i,x_j)$ the square Euclidean distance of the noisy image, $Z(x_i)$ is the normalization constant defined as follow:

$$Z(x_i)=\sum_{x_j\in\Omega^3}e^{\frac{-\left\|I(N_i)-I(N_j)\right\|_2^2}{h^2}} \quad (2)$$

$d^2_{ID}(x_i, x_j)$ is the square Euclidean distance of the new normalization image I_D ($I_D = div(D.\nabla I)$) [8], and h is a new modified smoothing parameter ($h = \beta.\hat{\sigma}_n$;where $\hat{\sigma}_n$ represent an unbiased estimation for Rician noise defined in [12]).

III. MRI SEGMENTATION

The segmentation is one of the most important parts of in MRI analysis. Most of the image segmentation research has focused on 2D images and the goal is to partition the slices of the MRI to different regions on given criteria. The most commonly used clustering algorithms for segmentation of images were the K-means and the Fuzzy c-means:

A. K-means

The k-means clustering method [13] partitions the input data into k classes by iteratively computing a mean intensity for each class which called centroid and segmenting the image by classifying each pixel/voxel in the class with the closest centroid obtained by minimizing the following objective:

$$V = \sum_{i=1}^{k} \sum_{x_j \in S_i} (x_j - \mu_i)^2 \tag{3}$$

Where k present the number of clusters and μ_i is the centroid or mean point of all the pixels $x_j \in S_i$ ($S_i = 1,2,3...k$)

B. Fuzzy c-means (FCM)

Fuzzy c-means (FCM) is a clustering method [16] based on the minimization of the following objective function:

$$J_{FCM} = \sum_{i=1}^{c} \sum_{j=1}^{n} m_{ij}^f d_{ik}^2 \tag{4}$$

Where c is the number of cluster centres; n is the number of data points; f is fuzzifier value (1 for hard clustering, and increasing for fuzzy clustering); m_{ik} is the fuzzy membership value of pixel k in cluster I; $d_{ik}^2 = \|x_k - v_i\|^2$ is the Euclidean distance; x_k is the k^{th} data points; v_i is the centroid of each cluster.

During clustering the FCM performs the following steps:

1. Set randomly the cluster membership values, μ_{ij}.
2. Calculate the cluster centres using the following equation:

$$m_{ij} = \frac{(\|x_i - v_k\|)^{-2/(m-1)}}{\sum_{j=1}^{n} (\|x_i - v_k\|)^{-2/(m-1)}} \tag{5}$$

$$v_k = \frac{\sum_{i=1}^{c} m_{ij}^f x_i}{\sum_{i=1}^{c} m_{ij}^f} \tag{6}$$

3. Update $m_{ij}(t+1)$.
4. Calculate the objective function, J_m.
5. Repeat steps 2–4 until J_m improves by less than a specified minimum threshold or until after a specified maximum number of iterations.

In the next section, we will give some experimental results in term of removing noise and segmentation methods with evaluation by quantitative measurements.

IV. EXPERIMENTAL RESULTS

First, we have evaluated our proposed denoising algorithm on realistic MRI phantom (Fig. 2) as a ground truth [20] with 1mm^3 resolution and volume size (181×217×181) a by computing a different quantitative index such as SSIM, PSNR and QILV [21] and then we have applied our algorithm on real data which was mentioned in detail in the paper [15].

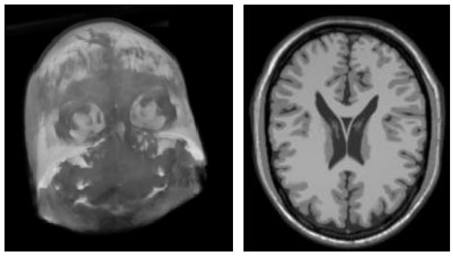

(a) (b)

Fig. 2 MRI phantom: (a) 3D Volume, (b) T1-weighted MR phantom slice.

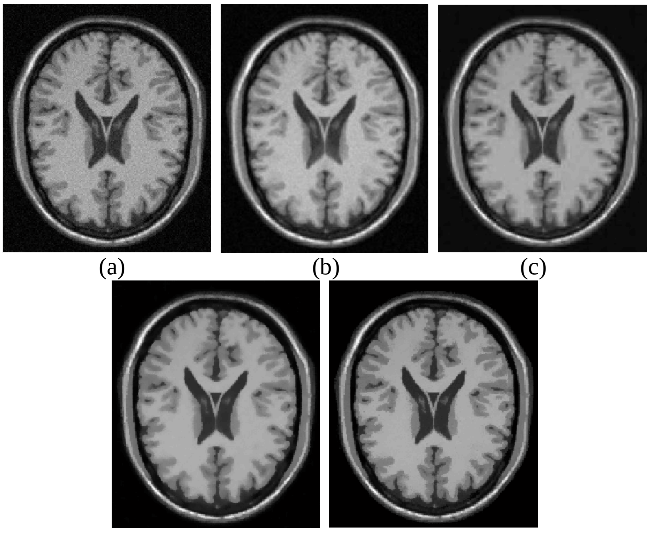

(a) (b) (c)

(d) (e)

Fig. 3 Experiment results on T1-weighted with 5% Rician noise added: (a) Noisy image, (b) TV denoised method, (c) Wavelet NeighShrinkSure denoised method, (d) PFNLM method, (e) Our Proposed method (3 iter).

The Fig. 3 present the denoising results for a T1-weighted MR phantom slice are contaminated with 5% Rician noise, followed by a TABLE I with the different results of quantitative measures such as SSIM, PSNR and QILV index compared to different methods like Total variation algorithm (TV) [19], Wavelet NeighShrink Sure method [17], a new normalization to the original NL-mean filter named PFNLM ("Polynomial-Fit" NLM) PFNLM [18]. Visually, as shown in Fig. 3 and Fig. 4, our proposed algorithm performs better than the others methods in term of preserving edges and removing noise and the quantitative values insure that.

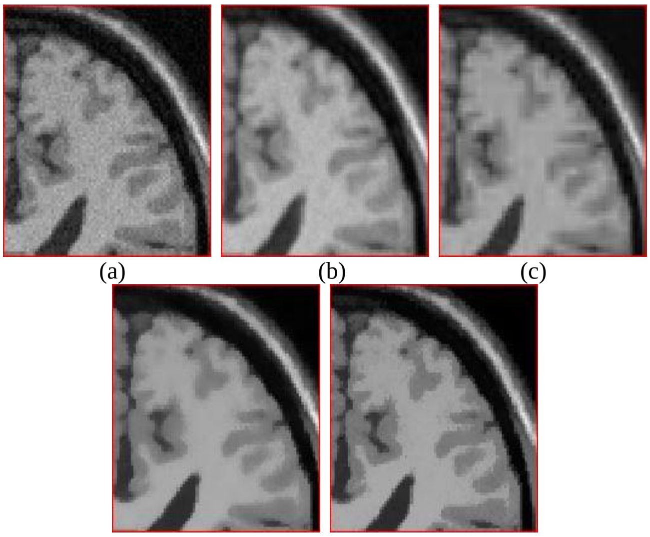

(a) (b) (c)

(d) (e)

Fig. 4 Details zoom on experiment results on T1-weighted with 5% Rician noise added: (a) Noisy image, (b) TV denoised method, (c) Wavelet NeighShrinkSure denoised method, (d) PFNLM method, (e) Our Proposed method.

TABLE I
COMPARISON OF DENOISING ALGORITHM OF T1-WEIGHTED WITH 5% AND 9% RICIAN NOISE

Algorithm	**SSIM**		**PSNR**		**QILV**	
	5%	**9%**	**5%**	**9%**	**5%**	**9%**
TV	0.66	0.58	16.68	14.94	0.77	0.73
NeighShrink Sure WT	0.73	0.66	27.71	24.75	0.90	0.78
PFNLM	0.73	**0.67**	27.72	24.86	0.93	0.84
Proposed	**0.74**	**0.67**	**28.02**	**24.91**	**0.94**	**0.89**

Other experimental result was presented in our paper [15] insure the performance of our algorithm compared to other methods. The following figures present the behaviour of our denoising method on segmentation task. So, first we segment the denoising slices with k-means clustering algorithm then with Fuzzy c-means clustering algorithm compared to over several estimators often used in the literature in order to judge the quality of the segmentation such as the Jaccard index, Dice index which measure the overlap between the segmentation obtained and the ground truth, false positive ratio which corresponds to the sensitivity and false negative ratio which corresponds to the specificity.

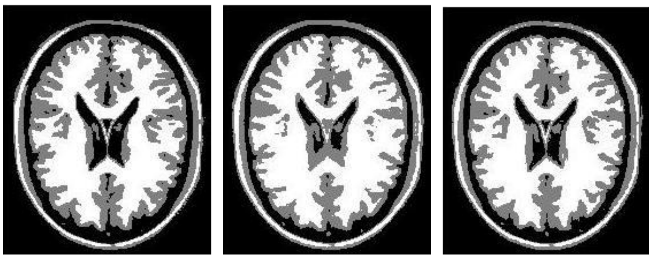

(a) (b) (c)

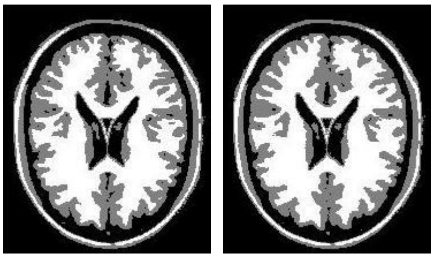

(d) (e)

Fig. 5 Kmeans segmentation for denoised MRI slice corrupted by 5% Rician noise: (a) Original T1-weighted slice, (b) TV denoised method, (c) Wavelet NeighShrinkSure denoised method, (d) PFNLM method, (e) Our Proposed method.

The Fig. 6 presents the result of Kmeans segmentation on T1-weighted slice denoised by different algorithms and the Fig.4 shows the Kmeans segmentation performance in term of Jaccard index, Dice index, False positive ratio and False negative ratio to different Rician noise levels.

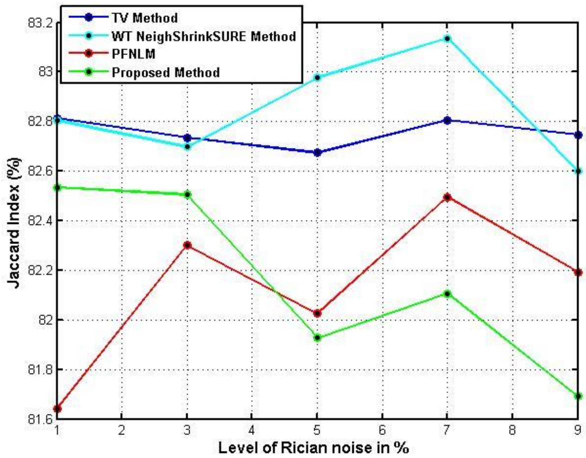

(a)

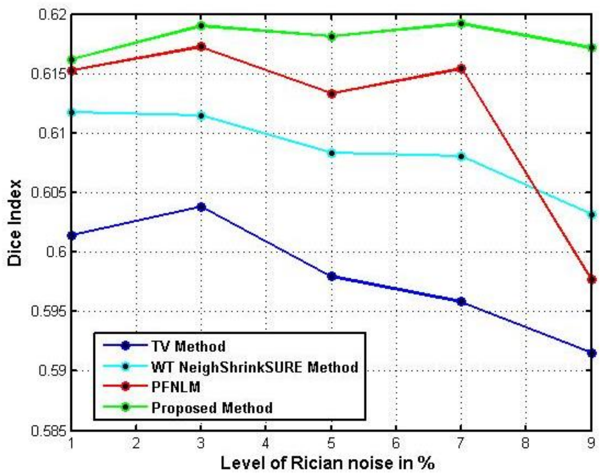

(b)

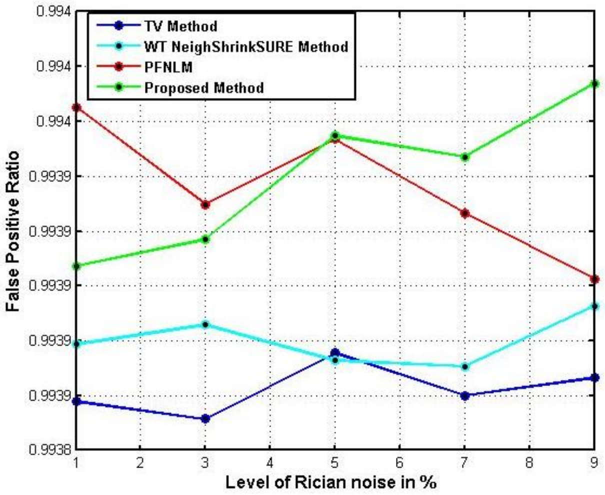

(c)

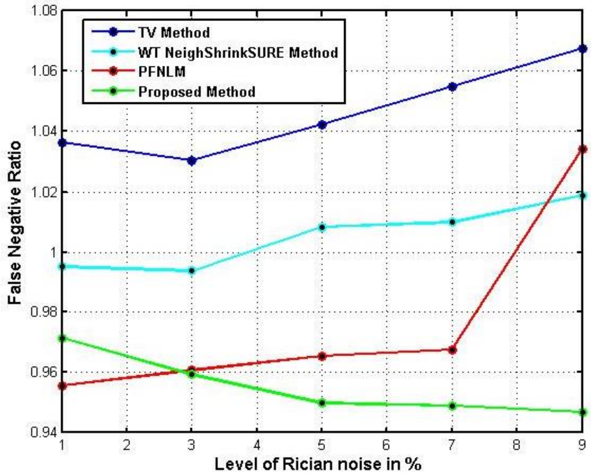

(d)

Fig. 6 Evaluation of the Kmeans segmentation : (a) Jaccard index for T1-weighted images with different Rician noise levels, (b) Dice index for T1-weighted images with different Rician noise levels, (c) False positive ratio for T1-weighted images with different Rician noise levels, (d) False negative ratio for T1-weighted images with different Rician noise levels.

The Fig. 7 presents the result of Fuzzy c-means segmentation on T1-weighted slice denoised by different algorithms and Fig. 8 shows the performance of Fuzzy c-means segmentation in term of quantitative measures for different Rician noise levels.

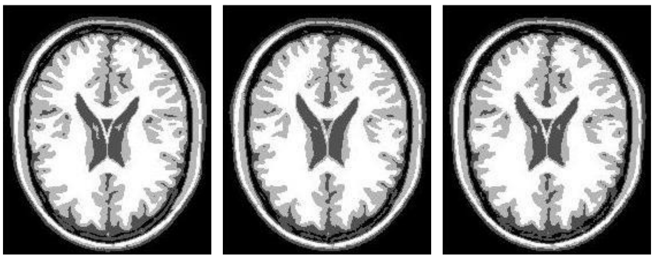

(a) (b) (c)

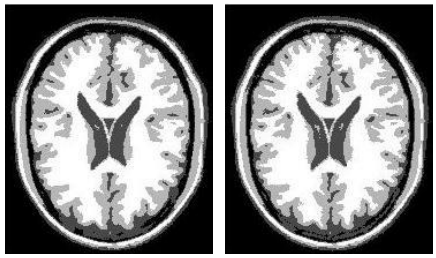

(d) (e)

Fig. 7 Fuzzy c-means segmentation for denoised MRI slice corrupted by 5% Rician noise: (a) Original T1-weighted slice, (b) TV denoised method, (c) Wavelet NeighShrinkSure denoised method, (d) PFNLM method, (e) Our Proposed method.

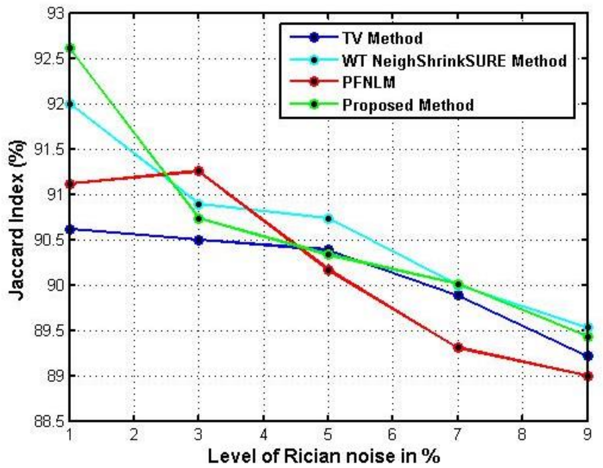

(a)

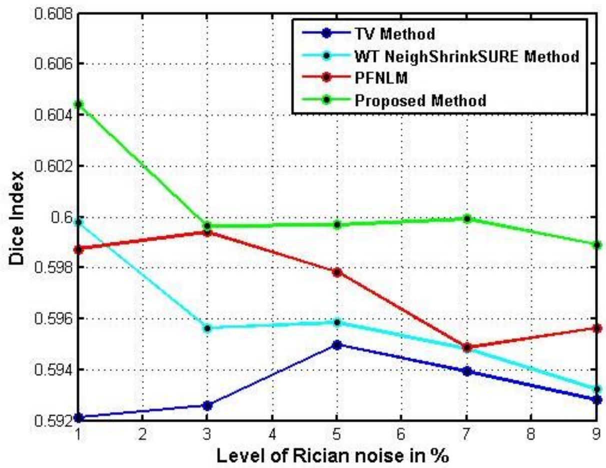

(b)

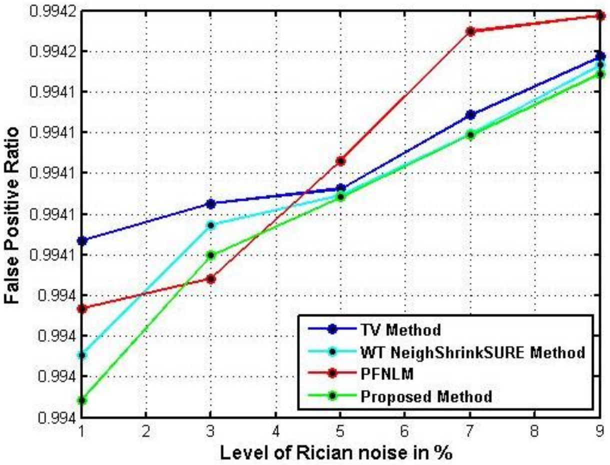

(c)

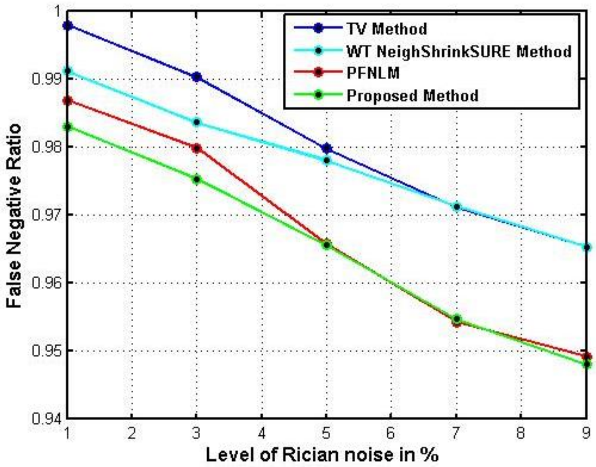

(d)

Fig. 8 Evaluation the Fuzzy c-means segmentation: (a) Jaccard index for T1-weighted images with different Rician noise levels, (b) Dice index for T1-weighted images with different Rician noise levels, (c) False positive ratio for T1-weighted images with different Rician noise levels, (d) False negative ratio for T1-weighted images with different Rician noise levels.

According to the Fig. 6 and Fig. 8, most of denoised algorithms perform better for low noise and for high noise the performance of our proposed algorithm remains good. Jaccard index present varying results, it's clear that our method have the lowest values in Kmeans segmentation but in the Fuzzy c-means segmentation our algorithm and the Wavelet NeighShrinkSure denoised method are performing approximately equal with higher values in different noise levels. In term of the false positive ratio, the results with lower value correspond to our algorithm which means that those parts of the image that are not presented neither in the result image nor in the ground truth image have low percentage. As well for false negative ratio, which contains those parts of the image that are not present in the result image but are present in the ground truth image, our algorithm have lowest values compared to the other denoising algorithms. Moreover, the Dice index (Fig.6 (b) and Fig. 8(b)) gives the highest values to our algorithm in both segmentation methods which greater than 50 % for the different noise levels.

.

V. CONCLUSION

In this paper, we compared the performance of our proposed algorithm and other 3D denoised methods such as TV, WT NeighShrinkSure and PFNLM models, in terms of slices segmentation. The experimental results on phantom data show a good performance of our proposed method based on the NL mean filter and the anisotropic diffusion tensor. In the future work we are looking to propose a new segmentation method combined to our denoised algorithm in order to control the smoothing task while removing noise in medical images.

REFERENCES

[1] Z. Chen and R. King, "Breast volume denoising and noise characterization by 3D wavelet transform". *ELSEVIER Computerized Medical Imaging and Graphics*,vol. 28, pp.235–246, 2004.

[2] M. Tran, R.Peteri, and M. Bergounioux, "Denoising 3D medical images using a second order variational model and wavelet shrinkage". *Image Analysis and Recognition*, vol. 7325, pp.138-145, Mar. 2012.

[3] A. Chambolle, P.L. Lions, "Image recovery via total variation minimization and related problems Numerische Mathematik ". *Journal of Mathematical Imaging and Vision*, vol.77(2), pp.167-188, Apr. 1997.

[4] M. Bergounioux, M.P. Tran "A second order model for 3D texture extraction". *Mathematical Image Processing. Springer proceedings in Mathematics 5*, 2011.

[5] E. Meijering, W. Niessen, J. Weickert, M. Viergever, "Diffusion-Enhanced Visualization and Quantification of Vascular Anomalies in Three-Dimensional Rotational Angiography: Results of an In-Vitro Evaluation". *Medical Image Analysis*, vol. 6(3), pp. 215–233, Sept. 2002.

[6] A. Mendrik, E. Vonken, A. Rutten, M. Viergever, B. van Ginneken. "Noise Reduction in Computed Tomography Scans using 3D Anisotropic Hybrid Diffusion with Continuous Switch". *IEEE Trans. Med. Imaging* , vol. 28(10),pp.1585–1594, Oct. 2009.

[7] A. Frangakis and R. Hegerl. "Noise reduction in electron tomographic reconstruction using nonlinear anisotropic diffusion". *Journal of Structural Biology*, vol. 135(3), pp.239-250, 2001.

[8] J. Weickert, B.M. ter Haar Romeny, M.A. Viergever, "Conservative Image Transformations with Restoration and Scale-Space Properties ", *Proceedings of the International Conference On Image Processing – ICIP-96*, vol. 1, pp. 465-468,1996.

[9] P. Coupé, P. Yger, S. Prima, P. Hellier, C. Kervrann, and C. Barillot, "An Optimized Blockwise NonLocal Means Denoising Filter for 3-D Magnetic Resonance Images*", IEEE Transactions on Medical Imaging*, vol. 27, pp. 425–441, Apr. 2008.

[10] L. He and I. R. Greenshields, "A Nonlocal Maximum Likelihood Estimation Method for Rician Noise Reduction in MR Images", *IEEE TMI*, vol. 28(2), pp. 165–172, 2009.

[11] P. Coupé, P. jpsé V. Manjon, Montserrat Robles and Louis Collins, "Adaptive Multiresolution Non-Local Means Filter for 3D MR Image Denoising", *IET image Processing*, 2011.

[12] H. Gudbjartsson and S. Patz, "The Rician Distribution of Noisy MRI Data", *Magn Reson Med*., vol. 34(6), pp. 910–914, Dec. 1995.

[13] J. MacQueen, "Some methods for classification and analysis of multivariate observations". *In Proc. Fifth Berkeley Sympos. Math. Statist. and Probability*, 1967.

[14] J.C. Bezdek, et al., "Fuzzy Models and Algorithms for Pattern Recognition and Image Processing", Springer, 2005.

[15] F. Romdhane, F. Benzarti, and H. Amiri. (*in press*), "A new method for denoising three-dimensional magnetic resonance images denoising". *Int. J. Computational Vision and Robotics*.

[16] B. Dawant, A. Zijidenbos, and R. Margolin, “Correction of intensity variations in M R images for computer-aided tissue classification”, *IEEE Transactions Medical Imaging*, vol. 12, pp. 770–781, 1993.
[17] Z. Dengwen and C. Wengang, “Image denoising with an optimal threshold and neighbouring window”, *Pattern Recogn Lett.*, Vol. 29, pp. 1694–1697. 2008.
[18] A.T. Vega, V.G. Pérez, S.A. Fernández and C.F. Westin, “Efficient and robust nonlocal means denoising of MR data based on salient features matching”, *Computer Methods and Programs in Biomedicine*, vol. 105, pp.131–144. 2012.
[19] L.I. Rudin, S. Osher,. and E. Fatemi, “Nonlinear total variation based noise removal algorithms”, *Physica D*, vol. 60, pp. 259-268, 1992.
[20] D.L. Collins., A.P. Zijdenbos, V. Kollokian, J.G. Sled, N.J. Kabani, C.J. Holmes, and A.C. Evans, “Design and construction of a realistic digital brain phantom”, *IEEE Transactions on Medical Imaging*, Vol. 17, pp. 463-468. 1998.
[21] S.A Fernández, R.S. Estépar, C.A. Lopez, and C.F. Westin, “Image Quality Assessment based on Local Varianc”, *Proceedings of the 28th IEEE EMBS Annual International Conference*. 2006.